PROCEEDINGS, Thirteenth Workshop on Geothermal Reservoir Engineering
Stanford University, Stanford, California, January 19-21, 1988
SGP-TR-113

PRESSURE INTERFERENCE DATA ANALYSIS FOR TWO-PHASE (WATER/STEAM) GEOTHERMAL RESERVOIRS

S. K. Garg and J. W. Pritchett

S-CUBED
P. O. Box 1620
La Jolla, California 92038-1620

ABSTRACT

A previously published approximate solution by Garg is used to develop a practical procedure for analyzing pressure interference (drawdown) data from a hot-water geothermal reservoir which evolves into a two-phase system as a result of fluid production. The observation well is assumed to remain in the single-phase (liquid) part of the reservoir. A numerical geothermal reservoir simulator is employed in a series of calculations to test the limits of applicability of the interpretation procedure. The numerical results suggest that the accuracy of the computed reservoir transmissivity depends somewhat on the size of the induced two-phase region. Even if the two-phase zone is extensive, the method can still be used to provide a good first approximation for the reservoir transmissivity; forward modeling with a numerical reservoir simulator may then be employed to refine the latter estimate for transmissivity. Numerical results also show that the observation well pressure buildup data will obey the superposition principle after the return of the reservoir to single-phase conditions.

INTRODUCTION

A geothermal system may be two-phase before production begins or may evolve into a two-phase system as a result of fluid production. Theoretical analyses of pressure drawdown and pressure buildup data for such systems have been published by Grant (1978), Garg (1980), Garg and Pritchett (1984), Moench and Atkinson (1978) and Sorey, *et al.* (1980); Riney and Garg (1985) applied these theoretical methods to analyze pressure buildup data from several wells which produced two-phase fluids. In contrast with these analyses of pressure drawdown and pressure buildup data from single wells, analysis of pressure interference data observed in nearby shut-in wells for two-phase (water/steam) systems has not yet been treated in the literature.

Pressure interference tests are essential for establishing reservoir connectivity and for computing interwell transmissivity. Planning and executing pressure interference tests in two-phase systems requires special considerations. As discussed by Grant and Sorey (1979), the effective compressibility of a two-phase system can be 100 to 10,000 times greater than the compressibilities of either water or steam alone; conversely, the effective diffusivity for a two-phase system is some 100 to 10,000 times smaller than that for single phase systems. This implies that it will take an inordinately long time to propagate pressure signals through a reservoir which is two-phase everywhere. Consequently, a pressure interference test in a system which is initially two-phase may well be impractical. A more interesting and tractable situation occurs when an initially single-phase reservoir evolves into a two-phase system as a result of fluid production. In the latter case, a boiling front propagates outward (during drawdown) from the producing wellbore; for all practical purposes, the boiling front may be treated as a constant pressure boundary (p = saturation pressure corresponding to the local reservoir temperature). The two-phase region is restricted to the neighborhood of the production well. Provided that the initial reservoir pressure is sufficiently high and that the two-phase region created during the drawdown phase is not too extensive, the entire reservoir will return to single-phase conditions sometime after the cessation of fluid production (see Garg and Pritchett, 1984).

In this paper, we restrict our attention to an initially single phase reservoir which evolves into a two-phase system as a result of fluid production. In addition, it will be assumed that the two-phase region is restricted to the neighborhood of the production well such that the observation well remains in the single-phase part of the reservoir. Our goal is to examine the character of the pressure signal to be expected at the observation well, and to develop practical methods for the analysis of this pressure signal to yield reservoir transmissivity and compressibility.

MATHEMATICAL MODEL

Garg (1980) considered the pressure response of an initially single-phase reservoir which evolves into a two-phase system on production. In this case, the reservoir is two-phase for $r > R$ [$R = R(t)$ denotes the location of the flash front] and is single phase for $r > R$. Consider a fully penetrating well located in an infinite reservoir of thickness h. Assuming that the skin factor is

zero, the pressure response for flow at a constant mass rate of production is given by (Garg, 1980):

$$0 < r < R: \; p = p_s + \frac{M \nu_t}{4\pi h k} \left\{ Ei \left[\frac{-r^2}{4t D_t} \right] - Ei \left[-\lambda^2 \right] \right\} \quad (1)$$

and

$$r > R: \; p = p_i + \frac{p_s - p_i}{Ei \left\{ -\lambda^2 D_t / D_\ell \right\}} \times Ei \left[\frac{-r^2}{4t D_\ell} \right] \quad (2)$$

where

$$R = 2\lambda \left[D_t \; t \right]^{1/2} \quad (3)$$

and λ is the root of

$$\frac{p_s - p_i}{Ei \left[-\lambda^2 D_t / D_\ell \right]} \times \exp \left[-\lambda^2 D_t / D_\ell \right] = \frac{M \nu_\ell}{4\pi h k} \exp \left[-\lambda^2 \right] \quad (4)$$

In Equations (1) to (4), we have employed the following notation:

D_ℓ = diffusivity for the liquid region

D_t = diffusivity for the two-phase region

h = formation thickness

k = absolute permeability

$k_{r\ell}(k_{rg})$ = liquid (gas) relative permeability

M = rate of mass production

p = pressure

p_i = initial formation pressure

p_s = saturation pressure

r = radius

t = time

$\nu_\ell(\nu_g)$ = liquid (gas) kinematic viscosity

ν_t = two-phase kinematic viscosity = $(k_{r\ell}/\nu_\ell + k_{rg}/\nu_g)^{-1}$

The liquid-region diffusivity D_ℓ is given by:

$$D_\ell = \frac{k}{\phi \rho_\ell \nu_\ell C} \quad (5)$$

where

ϕ = porosity

ρ_ℓ = liquid density

$C = C_m/\phi + C_\ell$

C_m = uniaxial formation compressibility

C_ℓ = liquid compressibility.

The effective diffusivity for the two-phase reservoir region can be written as:

$$D_t = \frac{k}{\phi \rho_t \nu_t C_t}, \quad (6)$$

where ρ_t and C_t denote the density of the flowing mixture and the compressibility of the two-phase region respectively. Given the flowing enthalpy H_t, the density of the flowing mixture ρ_t can be evaluated from:

$$\frac{1}{\rho_t} = \frac{H_g - H_t}{L \rho_\ell} + \frac{H_t - H_\ell}{L \rho_g} \quad (7)$$

where

H_g (H_ℓ) = Steam (liquid) enthalpy corresponding to the measured bottomhole pressure, and

L = Heat of vaporization.

For practical purposes, the two-phase compressibility C_t is given sufficiently accurately by the following approximate expression (Grant and Sorey, 1979)

$$\phi C_t = \langle \rho c \rangle \left[\frac{(\rho_\ell - \rho_g)}{L \rho_\ell \rho_g} \right]^2 (T + 273.15) \quad (8)$$

where

$$\langle \rho c \rangle \simeq (1 - \phi) \rho_r c_r + \phi \rho_\ell c_\ell \quad (9)$$

ρ_r = Intrinsic formation density

c_r (c_ℓ) = Specific heat for rock (liquid), and

T = Reservoir temperature.

For $4t D_t/r_w^2 > 100$ (here r_w denotes the well radius), Equation (1) can be approximated to give the following expression for bottomhole pressure, $p_w(t)$:

$$p_w(t) = p_s - \frac{M \nu_t}{4\pi k h} Ei(-\lambda^2)$$

$$- \frac{1.15 M \nu_t}{2\pi k h} \left\{ \log_{10} \frac{D_t t}{r_w^2} + 0.351 \right\} \quad (10)$$

Equation (10) implies that a plot of p_w versus $\log_{10} t$ should be a straight line and that the two-phase kinematic mobility k/ν_t is given by:

$$k/\nu_t = \frac{1.15 M}{2\pi h m} \quad (11)$$

where m denotes the slope of the straight line.

In deriving the above-described solution, Garg (1980) assumed that the two-phase region can be characterized by a constant kinematic mobility k/ν_t and a constant diffusivity D_t. In reality, the situation is much more complex. Both the kinematic mobility and diffusivity vary throughout the two-phase region. After an initial nonlinear period, $|\partial(k/\nu_t)/\partial r|$ and $|\partial D_t/\partial r|$ become small in a region adjoining the wellbore; and the bottomhole pressures are closely approximated by Equation (1). The situation is, however, completely different for large r ($r < R$); $|\partial(k/\nu_t)/\partial r|$ and $|\partial D_t/\partial r|$ remain finite near the flash front. It is thus not *a priori* obvious if Equation (1) provides an accurate solution for all values of r less than R. In that D_t is variable in the two-phase region, Equation (2) gives only an approximate solution for the pressure response in the single-phase region of the reservoir. Finally, it should be noted that Garg's solution is only valid for the drawdown phase. Because of nonlinear effects in two-phase flow, superposition cannot be used to compute the buildup response.

Despite the above-mentioned limitations, Garg's solution serves as a convenient point of departure for analyzing the observed pressure interference signal. In the following, it will be assumed that the reservoir fluid remains single-phase liquid in the vicinity of the observation well, and that *in situ* boiling is limited to a region surrounding the production well. Comparison of Equation (2) with the line source solution for a well producing a single-phase liquid (constant rate of mass production = M) shows that the two solutions become identical if $[p_s - p_i]/Ei\{-\lambda^2 D_t/D_\ell]$ in Equation (2) is replaced by $M \nu_\ell/4\pi kh$. Stated somewhat differently, the pressure response in the single-phase region (Equation 2) can be computed from the single-phase line source solution by replacing the actual flow rate M by an apparent flow rate M_{app}:

$$M_{app} = \frac{p_s - p_i}{Ei\left(-\lambda^2 D_t/D_\ell\right)} \cdot \frac{4\pi k h}{\nu_\ell} . \quad (12)$$

The apparent mass flow rate M_{app} is always less than the actual flow rate M. Because of the vast difference in the single- and two-phase compressibilities, a disproportionate share of the produced fluid comes from the two-phase region of the reservoir. This in turn implies that for identical rates of production the pressure drawdown at the observation well in the presence of *in situ* flashing will be less than that obtained in a liquid reservoir.

The preceding discussion suggests that the observed pressure interference signal may be analyzed in a straightforward manner provided a method was available for estimating the apparent mass flow rate M_{app}. Unfortunately, the calculation of M_{app} requires a knowledge of single-phase and two-phase diffusivities and the formation permeability. In that the latter quantities are the unknown parameters, it is not feasible to estimate M_{app} prior to solving Equations (1) through (11) for D_ℓ, D_t and k.

A perusal of Garg's solution suggests the following procedure for analyzing the pressure interference data:

1. Match the observed pressure interference signal to the line source type curve (see e.g. Earlougher (1977) for a discussion of the matching procedure). The matching procedure essentially involves (1) plotting observed pressure change Δp ($= p_i - p$) versus time t on a log-log scale and (2) overlaying the latter plot on the line source type curve. The type curve is a log-log plot of nondimensional pressure p_D versus a nondimensional similarity variable r_D^2/t_D,

$$p_D = -0.5\ Ei\ [-r_D^2/4\ t_D]. \quad (13)$$

2. Select a match point (p_D, Δp) and (r_D^2/t_D, t), and solve the following equations for X and D_ℓ:

$$-Ei(-X) = \frac{2\ (p_i - p_s)}{\Delta p}\ p_D \quad (14a)$$

$$t_D/r_D^2 = D_\ell\ t/r^2 \quad (14b)$$

where

$$X = \lambda^2\ D_t/D_\ell \quad (14c)$$

and r denotes the distance of the observation well from the production well. Here, it is assumed that the reservoir temperature T (and hence saturation pressure p_s) and initial pressure p_i are known from other measurements.

3. Calculate two-phase kinematic mobility k/ν_t from the observed pressure response in the production well. Compute two-phase diffusivity from Equations (6) through (9). Note that the calculation of D_t requires a knowledge of the enthalpy of the produced fluid in addition to formation porosity and thermal capacity.

4. Given X, D_ℓ and D_t, λ is computed from Equation (14c).

5. Formation transmissivity kh/ν_ℓ is then calculated from

$$kh/\nu_\ell = \frac{M}{4\pi} \exp(-\lambda^2) \cdot \frac{2\, p_D}{\Delta p} \exp(X). \quad (15)$$

An examination of the above-described procedure shows that the analysis of pressure interference data from two-phase reservoirs requires information from both the production and observation wells.

NUMERICAL RESULTS

In order to define the limits of applicability of the preceding theory, the THOR reservoir simulator (Pritchett, 1982) was exercised in one-dimensional radial configuration to generate a series of drawdown/buildup histories. The radially infinite reservoir is simulated using a 100 zone ($\Delta r_1 = \Delta r_2 = \ldots = \Delta r_{10} = 0.1$ m, $\Delta r_{11} = 1.15\ \Delta r_{10}$, $\Delta r_{12} = 1.15\ \Delta r_{11}$, ..., $\Delta r_{100} = 1.15\ \Delta r_{99}$) radial grid. The outer radius of the grid is 222,542 m and is sufficiently large such that no signal reaches this boundary during the time-scale of interest. We consider a fully penetrating well located in a reservoir of thickness h = 100 m. The well is represented as an integral part of the grid by assigning to the well-block (Zone 1) sufficiently high permeability and porosity; fluid production is specified as a mass sink in the well-block. No attempt is made here to treat wellbore storage effects; proper treatment of these effects would require the coupling of transient wellbore flow with the reservoir simulator. The reservoir rock properties selected are given in Table 1. The mixture (rock/fluid) thermal conductivity is approximated by Budiansky's formula (Pritchett, 1982). The initial fluid state for the three cases considered is shown in Table 2. The reservoir is produced at constant rate M (see Table 2 for values of M used) for $t = 10^6$ s and is then shut in for $\Delta t = 2 \times 10^6$ s. In all three cases, the reservoir is assumed initially to contain single-phase fluid at a temperature of 300°C; the initial formation pressure, however, varies from case to case. The saturation pressure corresponding to a temperature of 300°C is 8.5917 MPa. Thus, the initial pressure differs from the saturation pressure by 8.3 kPa, 108.3 kPa, and 408.3 kPa for Cases 1, 2 and 3 respectively. The observation well is assumed to be located at r = 192.202 m (center of grid zone 50).

TABLE 1

ROCK PROPERTIES EMPLOYED IN NUMERICAL SIMULATION

	Wellblock (i = 1)	Rock Matrix 2 ≤ i ≤ 100
Porosity, ϕ	0.9999	0.1000
Permeability k, m^2	5×10^{-11}	5×10^{-14}
Uniaxial Formation Compressibility C_m, MPa^{-1}	0	0
Rock Grain Density ρ_r, kg/m^3	1	2650
Rock Grain Thermal Conductivity K_r, W/m°C	0.00	5.25
Heat Capacity c_r, kJ/kg°C	0.001	1.00
Relative Permeabilities $k_{r\ell}$, k_{rg}	Straight-line*	Straight-line*
Residual Liquid Saturation $S_{\ell r}$	0.00	0.30
Residual Gas Saturation S_{gr}	0.00	0.05

* $K_{r\ell} = (S_\ell - s_{\ell r})/(1 - S_{\ell r})$ for $S_\ell \geq S_{\ell r}$

$K_{rg} = (S_g - S_{gr})/(1 - S_{gr})$ for $S_g \geq S_{gr}$.

TABLE 2

MASS PRODUCTION RATE M AND INITIAL FLUID STATE

Case No.	Production Rate M (kg/s)	Pressure MPa	Temperature °C
1	10	8.600	300
2	10	8.700	300
3	20	9.000	300

Along the saturation line, ASME Steam Tables (ASME, 1967) give the following values for liquid-water and steam density and enthalpy:

Liquid-water density ρ_ℓ = 712.5 kg/m^3

Steam density ρ_g = 46.20 kg/m^3

Liquid-water enthalpy H_ℓ = 1345 kJ/kg

Steam enthalpy H_g = 2749 kJ/kg

Latent heat of vaporization L = 1404 kJ/kg

Assuming that the specific heat for liquid water at initial reservoir conditions is ~ 5.2 kJ/kg°C, and employing the rock properties given in Table 1, we have:

$$<\rho c> = 0.9 \times 2650 \times 10^3 + 0.1 \times 712.5 \times 5.2\ 10^3 \sim 2.76\ 10^6\ J/m^3°C,$$

and

$$\phi C_t = <\rho c> \left[\frac{(\rho_\ell - \rho_g)}{L\ \rho_\ell\ \rho_g}\right]^2 (T + 273.15)$$

$$= 2.76 \left[\frac{712.5 - 46.2}{1404 \times 712.5 \times 46.2}\right]^2 (573.15)$$

$$= 3.29\ 10^{-7}\ Pa^{-1}.$$

Simulated drawdown histories at the production well for the three cases considered are shown in Figures 1 through 3. The drawdown data are seen to closely fit a straight-line in every case. The two-phase kinematic mobilities calculated from the slope of the straight line and Equation (11) are listed in Table 3. The simulated flowing enthalpies H_t were used along with Equations (6) through (8) to compute the flowing fluid densities ρ_t and two-phase diffusivities D_t (see Table 3 for numerical values).

Figures 4 through 6 display the simulated pressure drawdown (i.e. pressure interference) at the observation well; the simulated pressure interference data are seen to match the line-source solution closely. The match point in each case was used to compute the nondimensional parameter X (Equation 14a), the single-phase diffusivity D_ℓ (Equation 14b), and the nondimensional parameter λ (Equation 14c); the calculated values are displayed in Table 3.

Equation (3) implies that the flash-front propagates into the reservoir according to

$$R = At^{0.5},$$

where

$$A = 2\lambda\ D_t^{0.5}. \qquad (16)$$

Figures 7 through 9 show that the flash-front radius is indeed proportional to $t^{0.5}$. Table 3 compares the calculated values of A (Equation 16) with those obtained directly from Figures 7 through 9. The divergence between the computed (cf Equation 16) and actual values for A provides a measure of the adequacy of the theoretical solution. In view of the relatively

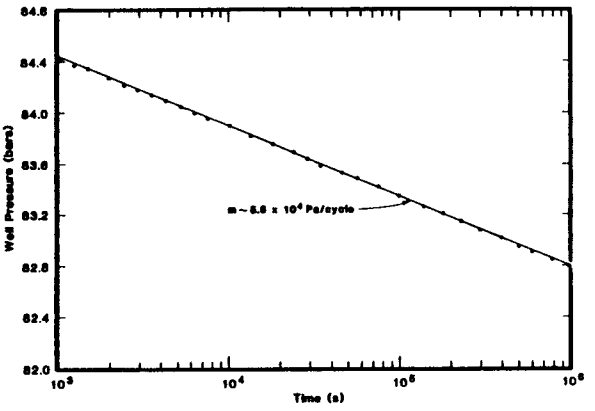

Figure 1. Simulated drawddown history (production well) for Case No. 1. Initial reservoir pressure and mass production rate are 8.600 MPa and 10 kg/s respectively.

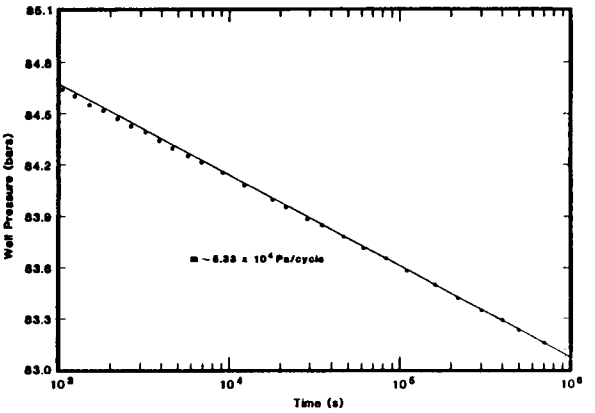

Figure 2. Simulated drawdown history (production well) for Case No. 2. Initial reservoir pressure and mass production rate are 8.700 MPa and 10 kg/s respectively.

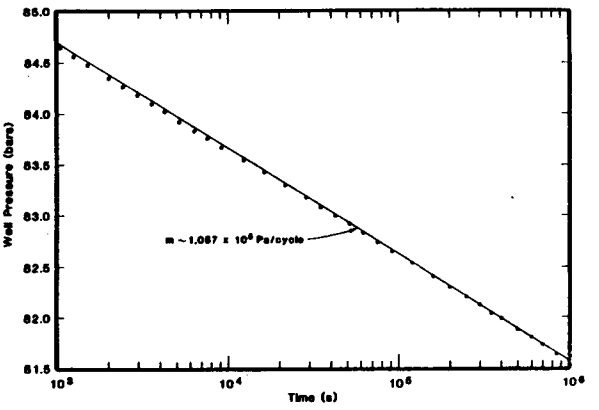

Figure 3. Simulated drawdown history (production well) for Case No. 3. Initial reservoir pressure and mass production rate are 9.000 MPa and 20 kg/s respectively.

TABLE 3

COMPUTATION OF RESERVOIR TRANSMISSIVITY kh/ν_ℓ AND APPARENT MASS FLOW RATE $M_{app.}$

Case No.	Two-Phase Kinematic Mobility k/ν_t (s)	Flowing Enthalpy H_t (kJ/kg)	Flowing Density ρ_t (kg/m^3)	Two-Phase Diffusivity D_t (m^2/s)	Single-Phase Diffusivity D_ℓ (m^2/s)	X $\lambda^2 D_t/D_\ell$ Nondim. *	λ Nondim.	$A_{calc.}$ ($m/s^{0.5}$) **	$A_{act.}$ ($m/s^{0.5}$)	Single-Phase Kinematic Transmissivity kh/ν_ℓ (m-s)	M_{app}/M ***
1	$3.33\ 10^{-7}$	1374.3	547.7	$1.85\ 10^{-3}$	2.364	$0.235\ 10^{-2}$	1.733	0.149	0.140	$2.61\ 10^{-5}$	0.05
2	$3.43\ 10^{-7}$	1360.0	617.4	$1.69\ 10^{-3}$	2.364	$0.356\ 10^{-3}$	0.7057	0.0580	0.0510	$3.29\ 10^{-5}$	0.61
3	$3.46\ 10^{-7}$	1346.5	701.7	$1.50\ 10^{-3}$	2.438	$0.1622\ 10^{-4}$	0.1624	0.0126	0.0114	$3.97\ 10^{-5}$	0.97

* See Equations (14a) and (14c)

** $A_{cal.} = 2\ \lambda\ D_t^{0.5}$

*** Equation (12)

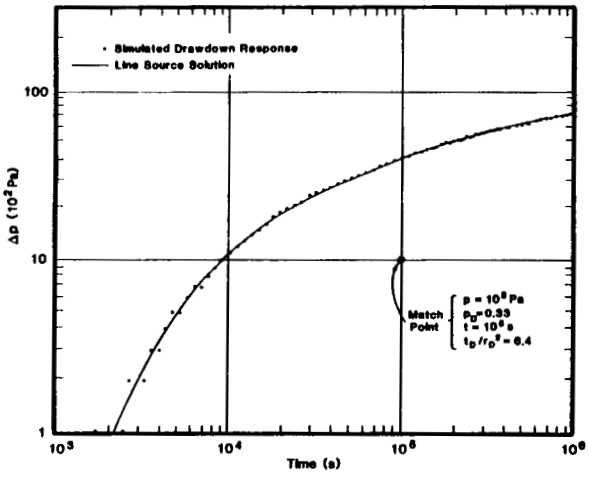

Figure 4. Match of the simulated pressure response at the observation well (r = 192.202 m) to the line-source solution (Case 1).

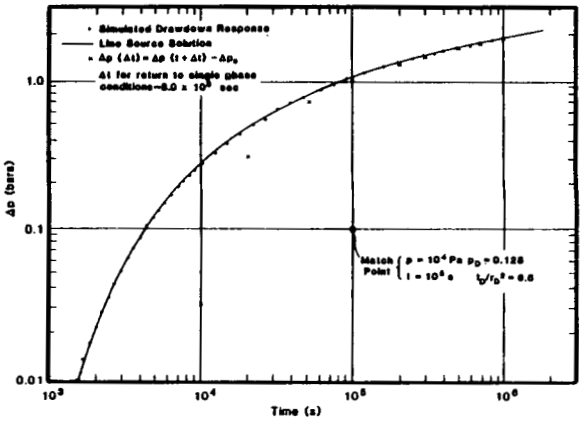

Figure 6. Match of the simulated pressure response at the observation well (r = 192.202 m) to the line-source solution (Case 3).

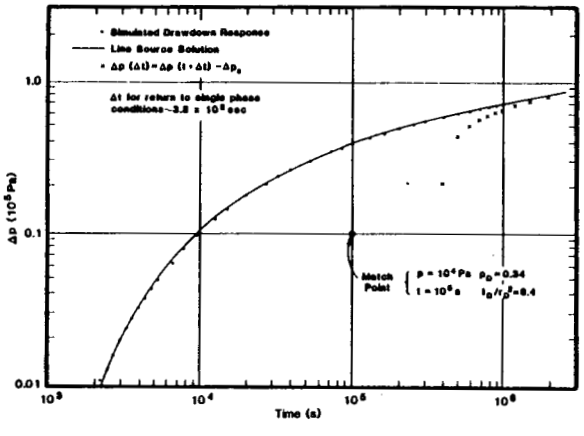

Figure 5. Match of the simulated pressure response at the observation well (r = 192.202 m) to the line-source solution (Case 2).

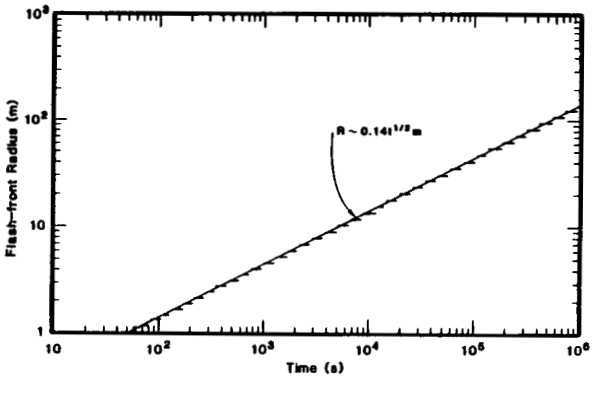

Figure 7. Flash-front radius versus drawdown time for Case No. 1.

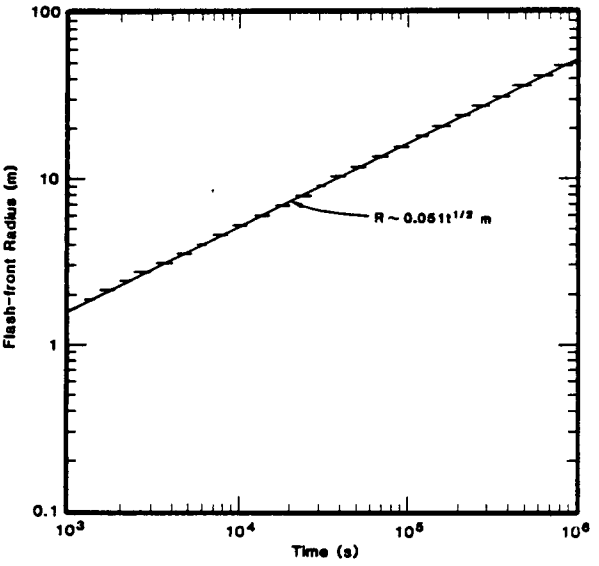

Figure 8. Flash-front radius versus drawdown time for Case No. 2.

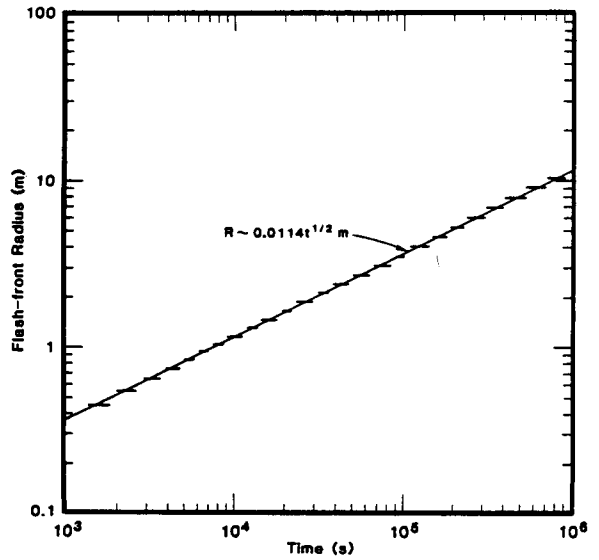

Figure 9. Flash-front radius versus drawdown time for Case No. 3.

small error in A (10 • 4 percent), one may be tempted to conclude that the linear solution should be sufficient for analyzing pressure interference data. This is, however, not always true. In that the nondimensional parameter λ occurs in the exponential term in Equation (15), a small error in A (and hence λ) can lead to a relatively large error in the calculated reservoir transmissivity.

Finally, the kinematic transmissivities kh/ν_ℓ (Equation 15) and the ratio of apparent flow rate M_{app} to the actual flow rate (Equation 12) are also given in Table 3. A comparison of the calculated transmissivities (Table 3) with the input value of $4.02\ 10^{-5}$ m-s shows that the agreement between the computed and the input values gets progressively worse as the two-phase effects become more pervasive. In Case 1, the computed value is only two-thirds of the actual transmissivity; note that in this case the apparent mass flow rate M_{app} is only ~ 5 percent of the input mass rate M. The latter results are to be contrasted with those for Case 3 wherein $M_{app}/M \sim 0.97$, and the computed value of kh/ν_ℓ is in close agreement with the input value. These numerical results suggest that the theoretical method of Section II can always be used (even in the presence of a large two-phase zone) to provide a first estimate for reservoir transmissivity. In cases wherein an extensive two-phase zone develops as a result of fluid production, it would seem prudent to check the computed value of kh/ν_ℓ by a forward simulation using a numerical reservoir simulator.

For a single-phase reservoir, superposition can be utilized to construct solutions for pressure buildup response. Thus, for a constant rate of mass production, the shutin pressure Δp_s at a time Δt after the cessation of production operations is given by:

$$\Delta p_s = \Delta p\ (t + \Delta t) - \Delta p\ (\Delta t), \qquad (17)$$

where $\Delta p\ (t + \Delta t)$ and $\Delta p(\Delta t)$ are the pressure drawdowns at times $(t + \Delta t)$ and Δt, respectively, computed from the line-source solution. Assuming that a match of the drawdown data to the line source solution is available, Equation (17) implies that

$$\Delta p\ (\Delta t) = \Delta p\ (t + \Delta t) - \Delta p_s\ . \qquad (18)$$

should also lie on the line source curve. Because of nonlinear effects in two-phase flow, superposition does not, strictly speaking, apply. Nevertheless, we decided to compute $\Delta p\ (\Delta t)$ (Equation 18) and to test the applicability (or lack thereof) of superposition empirically. Figures 5 and 6 (Cases 2 and 3) show that about one-half log cycle after the return of reservoir to single-phase conditions, the buildup data are closely approximated by the line-source solution. (In Case 1, the reservoir did not return to single-phase conditions during the time scale of interest. As a matter of fact, the two-phase zone advanced farther into the reservoir and engulfed the observation well. The buildup pressures in this case are quite different from those implied by Equation (18).) These results suggest that superposition may be used to model the pressure response of the observation well after the return of reservoir to single-phase conditions.

CONCLUDING REMARKS

The principal purpose of this paper is to develop a practical procedure for analyzing pressure interference data from a two-phase (water/steam) geothermal reservoir. It is assumed that the geothermal reservoir is initially all liquid and that the two-phase zone is created on initiation of production operations. The observation well is, however, assumed to always remain in the single-phase region of the reservoir. Garg (1980) derived an approximate solution for the pressure (drawdown) response of hot water reservoirs which undergo flashing on production. A numerical reservoir simulator was employed to test the applicability of the latter solution for analyzing pressure interference data. Application of the analysis procedure discussed in this paper requires pressure data from both the production and the observation wells in addition to information regarding the thermomechanical properties (i.e. specific heat, temperature, porosity, density, etc.) of the reservoir rocks. As far as the pressure drawdown response of the observation well is concerned, the effect of the two-phase zone can be represented by a reduced (or apparent) mass flow rate. The calculation of this apparent mass flow rate can, however, only be made after solving for reservoir transmissivity and diffusivity. If the two-phase zone created during drawdown is very large, then the apparent mass flow rate will be a small fraction of the actual production rate. In the latter case, the analytical method will yield only a first rough estimate of reservoir transmissivity; a more accurate estimate may then be obtained by forward modeling (history-matching) using a numerical reservoir simulator.

Because of nonlinear effects in two-phase flow, the superposition principle does not usually apply in two-phase problems. More specifically, Garg and Pritchett (1984) showed that the buildup response of the production well cannot be constructed from the drawdown solution. The numerical results in this paper, however, suggest that the buildup response of the observation well, subsequent to the return of the reservoir to single-phase conditions, does obey the superposition principle. The buildup data can, therefore, be used to check the consistency of formation properties derived from an analysis of drawdown pressures.

REFERENCES

ASME (1967), ASME Steam Tables, *The American Society of Mechanical Engineers*, New York.

Earlougher, R. C. (1977), Advances in Well Test Analysis, *Monograph Series, Vol. 5, Society of Petroleum Engineers*, Dallas.

Garg, S. K. (1980), "Pressure Transient Analysis for Two-Phase (Water/Steam) Geothermal Reservoirs," *Society of Petroleum Engineers Journal, Vol. 20*, pp. 206-214.

Garg, S. K. and J. W. Pritchett (1984), "Pressure Transient Analysis for Two-Phase Geothermal Wells: Some Numerical Results," *Water Resources Research, Vol. 20*. pp. 963-970.

Grant, M. A. (1978), "Two-Phase Linear Geothermal Pressure Transients: A Comparison With Single-Phase Transients," *New Zealand Journal of Science, Vol. 21*, pp. 355-364.

Grant, M. A. and M. L. Sorey (1979), "The Compressibility and Hydraulic Diffusivity of a Water-Steam Flow," *Water Resources Research, Vol. 15*, pp. 684-686.

Moench, A. F. and P. G. Atkinson (1978), "Transient Pressure Analysis in Geothermal Steam Reservoirs With an Immobile Vaporizing Liquid Phase," *Geothermics, Vol. 7*, pp. 253-264.

Pritchett, J. W. (1982), "User's Guide to the THOR Thermal Reservoir Simulator," S-CUBED Report No. SSS-R-83-5795.

Riney, T. D. and S. K. Garg (1985), "Pressure Buildup Analysis for Two-Phase Geothermal Wells: Application to the Baca Geothermal Field," *Water Resources Research, Vol. 21*, pp. 372-382.

Sorey, M. L., M. A. Grant and E. Bradford (1980), "Nonlinear Effects in Two-Phase Flow to Wells in Geothermal Reservoirs," *Water Resources Research, Vol. 16*, pp. 767-777.